

Postreceptor Neuronal Loss in Intermediate Age-related Macular Degeneration



ENRICO BORRELLI, NIZAR SALEH ABDELFAH, AKIHITO UJI, MUNESWAR GUPTA NITTALA, DAVID S. BOYER, AND SRINIVAS R. SADDA

- **PURPOSE:** To investigate the relationship between ganglion cell complex (GCC) thickness and photoreceptor alterations in eyes with intermediate age-related macular degeneration (AMD).
- **DESIGN:** Retrospective case-control study.
- **METHODS:** We collected data from 68 eyes with intermediate AMD from 68 patients with spectral-domain optical coherence tomography (SDOCT) imaging. A control group of 50 eyes from 50 healthy subjects was included for comparison. Our main outcome measures for comparison between groups were (1) the average and minimum GCC thickness and (2) the “normalized” reflectivity of the ellipsoid zone (EZ) en face image.
- **RESULTS:** The average and minimum GCC thicknesses were thinner in AMD patients ($69.54 \pm 9.30 \mu\text{m}$ and $63.22 \pm 14.11 \mu\text{m}$, respectively) than in healthy controls ($78.57 \pm 6.28 \mu\text{m}$ and $76.28 \pm 6.85 \mu\text{m}$, $P < .0001$ and $P < .0001$, respectively). Agreement was found to be excellent in the “normalized” EZ reflectivity assessment (intraclass correlation coefficient = 0.986, coefficient of variation = 1.11). The EZ “normalized” reflectivity was 0.67 ± 0.11 in controls and 0.61 ± 0.09 in the AMD group ($P = .006$). In univariate analysis, EZ “normalized” reflectivity was found to have a significant direct relationship with average ($P < .0001$) and minimum ($P < .0001$) GCC thickness in AMD patients, but not in controls ($P = .852$ and $P = .892$, respectively).
- **CONCLUSIONS:** Eyes with intermediate AMD exhibit GCC thinning, as well as a reduced EZ “normalized” reflectivity, and these parameters are correlated. This study supports the concept of postreceptor retinal neuronal loss as a contributor to retinal thinning in intermediate AMD. (Am J Ophthalmol 2017;181:1–11. © 2017 Elsevier Inc. All rights reserved.)

AGE-RELATED MACULAR DEGENERATION (AMD) IS the leading cause of irreversible central vision loss among older individuals in the Western world.¹ Early AMD is characterized by the accumulation of medium drusen and intermediate AMD is identified by the presence of large drusen and/or pigmentary abnormalities.² Although many factors have been implicated in the pathogenesis and progression of this disorder, AMD is fundamentally characterized by damage to the unit composed of the photoreceptors, retinal pigment epithelium (RPE), Bruch membrane, and choriocapillaris.^{3,4} The dysfunction of this unit leads to the development of drusen between the RPE and Bruch membrane and progressive photoreceptor, RPE, and choriocapillaris loss.^{5,6}

Although AMD is primarily considered to be an outer retinal disease, there is a strong body of evidence that suggest that the inner retinal layers are also affected from an early stage of the disease. Several studies have suggested reduced retinal perfusion in eyes with early or intermediate AMD, which may provide a potential explanation for a reduction in inner retinal cells via an ischemic mechanism.⁷ Other authors have speculated that a mechanical compression from the underlying drusen might also affect the inner retinal layers.⁸ Alternatively, photoreceptor death in AMD has been hypothesized to initiate a cascade of neuronal death and retinal remodeling. Several histopathologic studies give credence to the latter theory, also called the postreceptor functional loss hypothesis,^{9,10} although to our knowledge no study has investigated this relationship using an imaging approach.

Spectral-domain optical coherence tomography (SDOCT) has been widely used to evaluate eyes with early/intermediate AMD. Several groups have demonstrated that AMD can impact the thickness of the ganglion cell complex (GCC), which is composed of the inner plexiform layer (IPL) and ganglion cell layer (GCL).

En face OCT has revolutionized macular imaging. This technique allows topographic qualitative investigation and quantitative measurements of several parameters at various depth-resolved levels of the retina. The inner segment/outer segment (IS/OS) junction is typically characterized as a reflective layer, situated posterior to the weak-reflecting outer nuclear layer (ONL) and anterior to the strong-reflecting RPE. The reflection signal arising from the IS/OS junction has recently been suggested by some to originate from the photoreceptor IS ellipsoids,



Supplemental Material available at AJO.com.

Accepted for publication Jun 6, 2017.

From the Doheny Image Reading Center, Doheny Eye Institute, Los Angeles, California (E.B., N.S.A., A.U., M.G.N., S.R.S.); Department of Ophthalmology, David Geffen School of Medicine at UCLA, Los Angeles, California (E.B., N.S.A., A.U., M.G.N., S.R.S.); Ophthalmology Clinic, Department of Medicine and Science of Ageing, University G. D'Annunzio Chieti-Pescara, Chieti, Italy (E.B.); and Retina Vitreous Associates Medical Group, Beverly Hills, California (D.S.B.).

Inquiries to Srinivas R. Sadda, 1355 San Pablo St, Suite 211, Los Angeles, CA 90033; e-mail: SSadda@doheny.org

which are densely packed with mitochondria; thus the IS/OS junction is also termed the ellipsoid zone (EZ).¹¹ Discontinuities (breaks) in the IS/OS junction are seen as hyporeflective areas on the en face image. Thus it seems rational, and it has been demonstrated, that the reflectivity of the IS/OS junction might be a surrogate for photoreceptor damage.^{12,13}

In the present study, we investigated the reflectivity of the en face IS/OS slab in intermediate AMD eyes, with a method to generate an accurate and objective measurement. Our aim is to help shed further light on the relationship between GCC thickness and photoreceptor damage in intermediate AMD patients. This could be helpful to better understand the disease pathophysiology, as well as to identify potential biomarkers for disease progression and new targets for pharmacologic treatment.

METHODS

• **STUDY PARTICIPANTS:** In this retrospective case-control study, subjects aged 50 years and older with intermediate AMD² in 1 eye were identified from Doheny UCLA Eye Centers and OCT imaging data were exported for subsequent analysis at the Doheny Image Reading Center. The study was approved by the UCLA Institutional Review Board and adhered to the tenets of the Declaration of Helsinki and the Health Insurance Portability and Accountability Act. An informed consent waiver was granted to allow retrospective analysis of the previously collected data.

To be included in this analysis, patients had to have been imaged with the Cirrus HD-OCT (Carl Zeiss Meditec, Inc, Dublin, California, USA) between January 2009 and January 2014. Moreover, all patients underwent a complete ophthalmologic examination, which included the measurement of best-corrected visual acuity (BCVA), intraocular pressure (IOP), and dilated fundus examination. Medical history, including diabetes status, was collected for each patient.

The inclusion criteria for AMD eyes included having drusen >125 μm in diameter with or without pigmentary abnormalities as assessed by clinical examination and confirmed by dense-volume OCT (pigment abnormalities on OCT manifesting as intraretinal hyperreflective features). In our cohort, all the fellow eyes were affected by wet AMD, in order to avoid the status of the fellow eye from confounding the analysis. Exclusion criteria for enrolled eyes were as follows: (1) presence of pseudodrusen on the OCT scan; (2) previous vitreoretinal surgery or anti-vascular endothelial growth factor (VEGF) injection; (3) any maculopathy secondary to causes other than AMD (including presence of an epiretinal membrane or vitreomacular traction syndrome); (4) refractive error greater than 3.00 diopters; (5) intraocular pressure >20 mm Hg;

(6) diagnosis of diabetic retinopathy; and (7) any optic neuropathy, including glaucoma. Furthermore, we excluded poor-quality images (signal strength <6) with either significant artifact or incorrect segmentation at the level of the GCC and/or IS/OS junction.

A control group of a similar age was also included in the current analysis. All control subjects were volunteers with no evidence of optic nerve and retinal disease, as evaluated by dilated fundus examination and OCT. In the control group, if both eyes were eligible for the study, only the right eye was included in the analysis.

BCVA measurements were made using a Snellen chart and were converted to the logarithm of the minimum angle of resolution (logMAR), as previously described.¹⁴

• **IMAGING:** All patients underwent macular cube 512×128 scan protocol covering a 6×6 -mm macular cube area centered on the fovea.

The ganglion cell analysis (GCA) algorithm (Cirrus OCT software, version 6.0) was used to detect and measure GCC thickness within an elliptical annulus around the fovea (dimensions: vertical inner and outer radii of 0.5 and 2.0 mm, respectively; horizontal inner and outer radii of 0.6 and 2.4 mm, respectively). The GCA algorithm identified and calculated the difference between the retinal nerve fiber layer (RNFL) and IPL outer boundary segmentations, and yielded the combined thickness of the GCL and IPL.^{15,16} The average and minimum GCC thicknesses were considered for this analysis. The software compares the thickness values against a normal age-matched database to assess whether the subject's GCC thickness values are normal ($P = 5\%–95\%$), borderline ($P = 1\%–5\%$), or reduced ($P < 1\%$ in the normal distribution).¹⁷

The drusen area and volume data used in this study for analysis were automatically generated by the Cirrus OCT software. The drusen thickness map was defined as the difference between the actual RPE segmentation and the RPE floor. This drusen thickness map is generated from each of the 40 000 data points and was automatically calculated, as previously reported.^{18,19} Drusen area and volume measurements were obtained for the macular area within circles centered on the fovea with diameters of 3 and 5 mm.

As the repeatability for GCA and drusen algorithms have been reported previously,^{20–22} the reproducibility was not reassessed in the present study.

• **EN FACE INNER SEGMENT/OUTER SEGMENT JUNCTION IMAGE PROCESSING:** For each patient, we first exported the en face image of the IS/OS junction (slab 21 μm thick with inner boundary located 45 μm above the RPE reference).

Despite the standardized acquisition techniques and the use of artificial tears to ameliorate ocular surface factors before scan acquisition, the signal quality and absolute brightness of structures visualized by OCT may still be

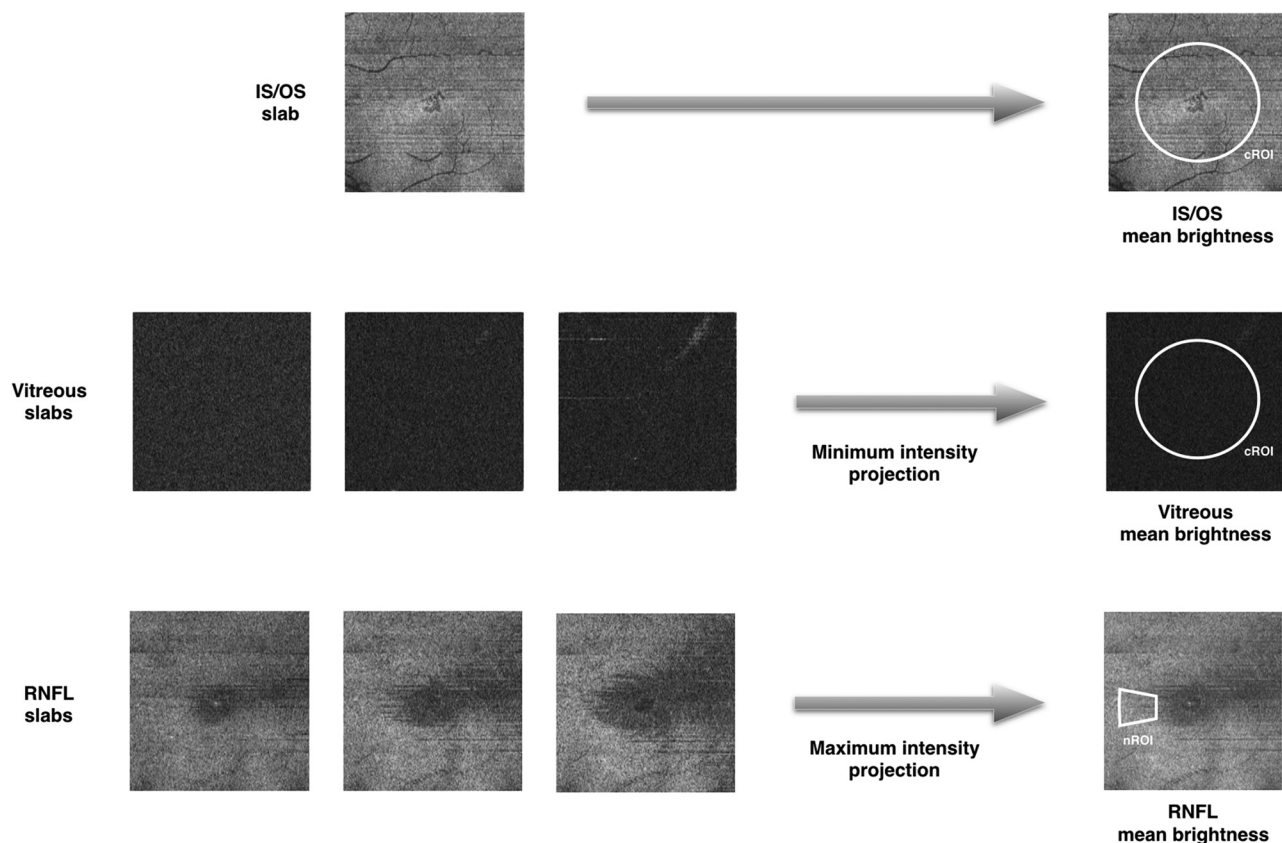


FIGURE 1. Representation of the algorithm used to test the inner segment/outer segment (IS/OS) “normalized” reflectivity. To evaluate the “normalized” IS/OS reflectivity we used the following 7 images: (1) the en face image of the IS/OS junction (slab 21 μm thick with the inner boundary located 45 μm above the retinal pigment epithelium reference); (2) 3 consecutive en face images from the vitreous (set with inner boundary located 4, 10, and 16 μm above the inner limiting membrane [ILM], respectively); and (3) 3 consecutive en face images from the retinal nerve fiber layer (RNFL; set with inner boundary at 8, 14, and 20 μm below the ILM, respectively). The mean brightness of the IS/OS junction image was calculated as the mean of all the pixel values in a circle region of interest (cROI) centered on the fovea. The mean vitreous brightness was tested in the cROI after the “minimum intensity” projection function was applied on the 3 vitreous imported images. The RNFL brightness was tested only in those RNFL pixels in an ROI centered on the nasal sector (nROI), where it is known the brightness is higher, after applying the “maximum intensity” projection on the 3 exported images. Finally, the “normalized” IS/OS reflectivity was obtained by subtracting the vitreous brightness from the IS/OS brightness and dividing the remainder by the mean RNFL brightness.

affected by a variety of uncontrollable factors, such as media opacity. We previously described methods to normalize the signal between visits and patients, to allow more reliable comparisons of tissue brightness or reflectivity.^{23–25} The image processing algorithm we designed to normalize the IS/OS reflectivity (Figure 1) uses 2 reference structures, the vitreous and the RNFL, which constitute a dark and a bright reference standard, respectively.

Then, to compute a normalized brightness value for IS/OS reflectivity, we also exported the following 6 slabs, each with a thickness of 1 pixel: (1) 3 consecutive en face images from the vitreous (set with the inner boundary located 4, 10, and 16 μm above the inner limiting membrane [ILM], respectively); and (2) 3 consecutive en face images from the RNFL (set with the inner boundary at 8, 14, and 20 μm below the ILM, respectively). The decision

to export 3 images for each of the 2 reference structures was taken in order to minimize the risk of segmentation errors confounding the analysis. Furthermore, 2 Doheny Image Reading Center–certified OCT graders (E.B. and A.U.) reviewed all exported en face OCT images (1 from the IS/OS slab, 3 from the vitreous, and 3 from the RNFL) to confirm the absence of artifacts (eg, motion) before analysis.

The obtained 7 images for each patient were then imported into image analysis ImageJ software (version 1.50; National Institutes of Health, Bethesda, Maryland, USA; available at <http://rsb.info.nih.gov/ij/index.html>). The mean brightness of the IS/OS junction image was calculated as the mean of all the pixel values (considering that each pixel in the 8-bit exported image may be in a grayscale range of possible values from 0 to 255, where typically 0 is

TABLE 1. Demographic and Clinical Characteristics of Controls and Age-related Macular Degeneration Patients

	Control	AMD		
		Overall	Normal GCC ^a	Abnormal GCC ^a
Number of eyes	50	68	43	25
Age (y), mean ± SD	70.9 ± 8.1	79.8 ± 7.6	78.8 ± 8.3	81.4 ± 6.2
Sex, n				
Male	12	23	14	9
Female	38	45	29	16
BCVA (logMAR), mean ± SD	0.00 ± 0.00	0.22 ± 0.18	0.16 ± 0.02	0.28 ± 0.22
Diabetes, n	5	12	7	5

AMD = age-related macular degeneration; BCVA = best-corrected visual acuity; GCC = ganglion cell complex; logMAR = logarithm of the minimum angle of resolution; SD = standard deviation.

^aAbnormal GCC indicates patients with a borderline/reduced average GCC thickness; Normal GCC indicates patients with a normal average GCC thickness.

taken to be black and 255 is taken to be white) in a circle region of interest (cROI) centered on the fovea (dimensions: radius of 2 mm, area of 12.56 mm², respectively). This choice was taken based on the limited lateral resolution of the en face OCT images. To obtain the final normalized IS/OS reflectivity, first the mean brightness (or optical density) of the vitreous is subtracted, and the remainder is then divided by the mean brightness of the nasal RNFL, as indicated in the following formula:

$$\frac{IS}{OS} \text{ normalized reflectivity} = \frac{\frac{IS}{OS} \text{ mean brightness [cROI]} - \text{Vitreous mean brightness [cROI]}}{RNFL \text{ mean brightness [nROI]}} \quad (1)$$

To obtain the mean vitreous brightness, we first used the ImageJ “minimum intensity” projection function on the 3 vitreous imported images. Thus, we tested the intensity on the obtained image by using only those vitreous pixels in the cROI. To obtain the mean RNFL brightness, the 3 RNFL imported images underwent the “maximum intensity” projection process. Then, we tested the intensity by using only those RNFL pixels in an ROI centered on the nasal sector (nROI; area of 1.11 mm²), where it is known that the brightness is higher.

• **STATISTICAL ANALYSIS:** To detect departures from normality distribution, a Shapiro-Wilk test was performed for all variables. Means and standard deviation (SD) were computed for all quantitative variables. Continuous variables were compared by conducting a 1-way analysis of covariance (ANCOVA) with Bonferroni post hoc test, by introducing age and diabetes as covariates.

The relationship between GCC thickness (dependent variable) and other OCT variables was investigated with a linear regression analysis. Since multiple linear regression

analysis allows us to estimate the association between a given dependent variable and other parameters, it provides a way of adjusting for (or accounting for) potentially confounding variables. Thus, subsequently, a multiple regression analysis with GCC average thickness as the dependent variable was applied, adjusting for age, sex, diabetes, scan strength, and drusen volume and area.

The 2-way mixed, average measure intraclass correlation coefficient (ICC) was calculated on 20 randomly selected

AMD eyes, in order to assess interobserver variation in assessing “normalized” IS/OS reflectivity. Furthermore, the coefficient of variation of absolute difference between graders was calculated.

Statistical calculations were performed using Statistical Package for Social Sciences (version 20.0, SPSS Inc, Chicago, Illinois, USA). The chosen level of statistical significance was $P < .05$.

RESULTS

• **CHARACTERISTICS OF PATIENTS INCLUDED IN THE ANALYSIS:** Of the 118 patients included in this analysis, 68 had intermediate AMD in 1 eye and 50 were healthy controls. The overall demographic and clinical characteristics of the 2 groups are shown in Table 1.

The AMD cohort was further divided into 2 subgroups according to the status of the average GCC thickness (normal, borderline/reduced). Forty-three eyes showed

TABLE 2. Tested Optical Coherence Tomography Variables in Controls and Age-related Macular Degeneration Patients

	Control	AMD	P Value
Average GCC thickness (μm)	78.57 \pm 6.28	69.54 \pm 9.30	<.0001
Minimum GCC thickness (μm)	76.28 \pm 6.85	63.22 \pm 14.11	<.0001
Vitreous brightness (gray level)	42.60 \pm 5.29	40.88 \pm 7.39	.236
RNFL brightness (gray level)	138.05 \pm 15.95	138.13 \pm 14.44	.326
IS/OS “normalized” reflectivity	0.67 \pm 0.11	0.61 \pm 0.09	.006
Drusen area (mm^2)			
3-mm	-	0.52 \pm 0.61	-
5-mm	-	0.68 \pm 0.77	-
Drusen volume (mm^3)			
3-mm	-	0.02 \pm 0.04	-
5-mm	-	0.03 \pm 0.04	-
Scan signal strength	7.7 \pm 1.3	7.8 \pm 1.3	.957

AMD = age-related macular degeneration; GCC = ganglion cell complex; IS/OS = inner segment/outer segment junction; RNFL = retinal nerve fiber layer.

Values were compared by 1-way analysis of covariance with age and diabetes as covariates, followed by Bonferroni post hoc test.

normal average GCC thickness (normal GCC group); 25 eyes were characterized by borderline/reduced average GCC thickness (abnormal GCC group).

• **ONE-WAY ANALYSIS OF COVARIANCE ANALYSIS:** Both the average and minimum GCC thicknesses were thinner in AMD patients (69.54 \pm 9.30 μm and 63.22 \pm 14.11 μm , respectively) compared to healthy controls (78.57 \pm 6.28 μm and 76.28 \pm 6.85 μm , $P < .0001$ and $P < .0001$, respectively) (Table 2).

The IS/OS junction “normalized” reflectivity was 0.67 \pm 0.11 in controls and 0.61 \pm 0.09 in the AMD group ($P = .006$) (Table 2). Interestingly, when the 2 AMD subgroups were considered, the IS/OS “normalized” reflectivity was decreased only in the abnormal GCC group (0.55 \pm 0.09), which was lower than both the normal GCC group (0.64 \pm 0.08, $P = .004$) and the control group (0.67 \pm 0.11, $P < .0001$) (Table 3, Figures 2 and 3).

Neither the area nor the volume of the drusen differed among the AMD groups.

The vitreous and RNFL brightness, as well as the scan signal strength, did not show any difference between the groups, perhaps reflecting a consistency in the acquisition and analysis procedures.

• **REGRESSION ANALYSIS:** In univariate analysis, the “normalized” IS/OS reflectivity was found to have a significant direct relationship with average ($P < .0001$) and minimum ($P < .0001$) GCC thickness in AMD patients, but not in controls ($P = .852$ and $P = .892$, respectively) (Figure 4).

Area and drusen volume data were statistically not associated with GCC thickness by univariate regression analysis ($P = .995$ and $P = .656$ for drusen area variables, $P = .834$ and $P = .506$ for drusen volume variables, respectively).

In multiple regression analysis, IS/OS “normalized” reflectivity was significantly associated with average GCC thickness only in AMD patients ($P < .0001$) (Table 4).

• **INTEROBSERVER AGREEMENT:** Agreement was found to be excellent in the “normalized” IS/OS reflectivity assessment (ICC = 0.986, coefficient of variation = 1.11).

DISCUSSION

IN THIS CROSS-SECTIONAL STUDY WE INVESTIGATED GCC thickness and IS/OS reflectivity in normal and intermediate AMD eyes. Overall we found a strong relationship between GCC thickness and IS/OS “normalized” reflectivity in intermediate AMD eyes, while no relationship between these 2 parameters was seen in healthy eyes. Therefore, our results suggest that in AMD there appears to be some pathologic dependence between these 2 neuroretinal structures, at least on OCT. Because the purpose of our study was to investigate the relationship between inner and outer retinal layers in intermediate AMD eyes, we did not include eyes with late AMD. The impact of choroidal neovascularization and geographic atrophy on the inner retina has been evaluated in previous reports.^{26,27}

Several authors have investigated the GCC and RNFL thicknesses in eyes with AMD. All of these studies demonstrated a GCC thinning since the earliest stages, while the RNFL thickness was conserved in these early/intermediate AMD eyes.^{8,28,29} Furthermore, Hwang³⁰ demonstrated that the GCC thinning in AMD eyes has a peculiar pattern and is located around the fovea in a ring-shaped area. We confirmed that the inner retinal layers are affected in intermediate AMD, and this reduction does not appear to be influenced by age.

TABLE 3. Tested Optical Coherence Tomography Variables in Controls and in the 2 Age-related Macular Degeneration Groups

	Normal	AMD	
		Normal GCC ^a	Abnormal GCC ^a
Average GCC thickness (μm)	78.57 ± 6.28	74.51 ± 4.38 .467 ^b	61.00 ± 9.38 < .0001 ^b < .0001 ^c
Minimum GCC thickness (μm)	76.28 ± 6.85	70.28 ± 6.24 .770 ^b	51.08 ± 15.64 < .0001 ^b < .0001 ^c
Vitreous brightness (gray level)	42.60 ± 5.29	39.91 ± 6.17 .284 ^b	42.54 ± 9.01 1.0 ^b .267 ^c
RNFL brightness (gray level)	138.05 ± 15.95	139.59 ± 13.64 .734 ^b	135.61 ± 15.69 1.0 ^b 1.0 ^c
IS/OS “normalized” reflectivity	0.67 ± 0.11	0.64 ± 0.08 1.0 ^b	0.55 ± 0.09 < .0001 ^b .004 ^c
Drusen area (mm ²)			
3-mm	-	0.46 ± 0.61	0.61 ± 0.60 .159 ^c
5-mm	-	0.61 ± 0.79	0.81 ± 0.71 .293 ^c
Drusen volume (mm ³)			
3-mm	-	0.02 ± 0.03	0.03 ± 0.04 .212 ^c
5-mm	-	0.02 ± 0.03	0.04 ± 0.05 .075 ^c
Scan signal strength	7.7 ± 1.3	8.0 ± 1.3 1.0 ^b	7.4 ± 1.2 .932 ^b .325 ^c

AMD = age-related macular degeneration; GCC = ganglion cell complex; IS/OS = inner segment/outer segment junction; RNFL = retinal nerve fiber layer.

Values were compared by 1-way analysis of covariance with age and diabetes as covariates, followed by Bonferroni post hoc test.

^aAbnormal GCC indicates patients with a borderline/reduced average GCC thickness; Normal GCC indicates patients with a normal average GCC thickness.

^bComparison vs controls.

^cComparison vs normal GCC.

There are at least 3 potential hypotheses that may explain the involvement of the innermost retinal layers in AMD: (1) postreceptor functional loss, (2) postreceptor ischemia,³¹ and (3) mechanical tension.⁸ According to the postreceptor functional loss hypothesis, the neuronal damage may be caused by disorganized synaptic architecture and transneuronal degeneration over time, owing to the chronically reduced input to the inner retina secondary to the photoreceptor damage.^{9,10} Sullivan and associates¹⁰ conducted experiments on retinas obtained postmortem from eyes that had been affected by early/intermediate AMD, and demonstrated that inner retinal neurons either die or readily migrate out of the retina in response to the degeneration of photoreceptors.

To the best of our knowledge, there are no imaging-based studies that have evaluated the relationship between

inner retinal thickness and photoreceptor damage in intermediate AMD eyes.

To quantify the damage of the IS/OS junction, we tested the reflectivity of the OCT en face scan segmented at the level of the IS/OS junction. On en face OCT, the IS/OS discontinuities appear as darker areas within the highly reflective background. The break edges vary from sharp to indistinct, corresponding to a sudden discontinuity or gradual loss of reflectivity, respectively.³² Thus, it seems rational that photoreceptor discontinuity leads to a reduction in the IS/OS slab reflectivity. Investigation of the IS/OS junction reflectivity on en face OCT has been used to evaluate photoreceptor structure in macular telangiectasia (MacTel) type 2,³² macular hole,^{33,34} and AMD.^{13,35} In a previous paper, our group demonstrated that a lower

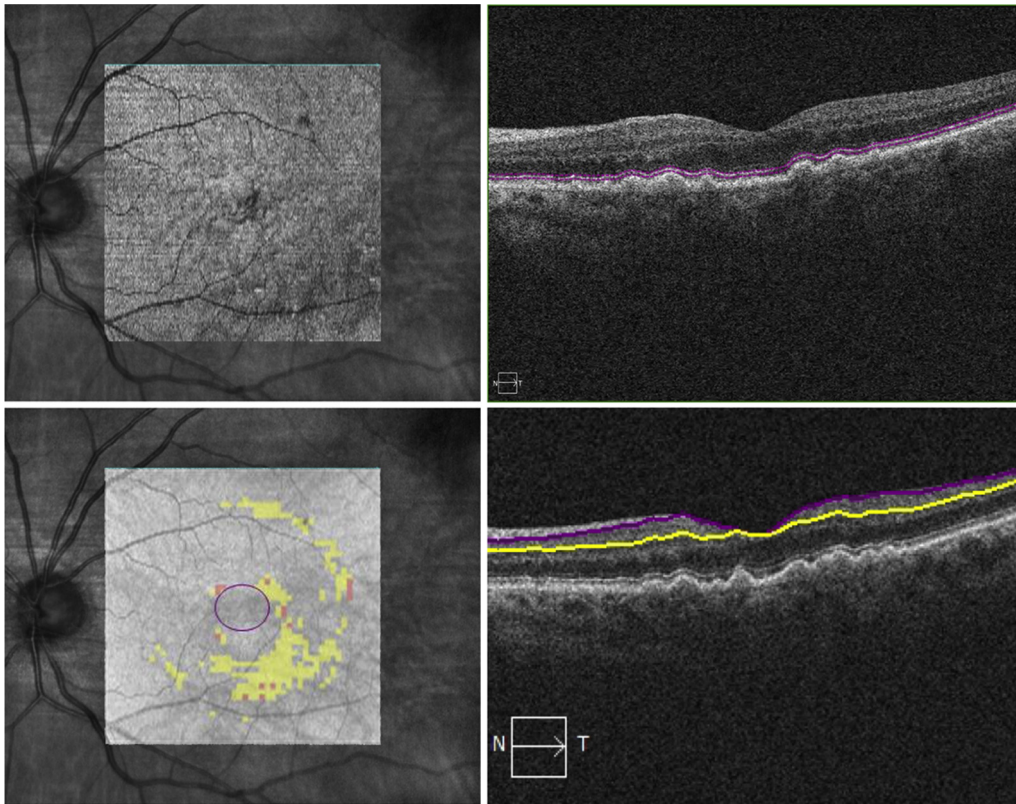


FIGURE 2. Representative optical coherence tomography (OCT) of a 72-year-old woman from the normal ganglion cell complex (GCC) group. (Upper left) En face 6 × 6-mm inner segment/outer segment (IS/OS) junction OCT overlaid onto line-scan ophthalmoscope (LSO) fundus image. (Upper right) Corresponding OCT B-scan showing the slab set to visualize the IS/OS image: 21 μm thick with the inner boundary located 45 μm above the RPE reference. (Lower left) En face 6 × 6-mm structural OCT with GCC deviation map overlaid onto LSO fundus image. (Lower right) Corresponding OCT B-scan showing the segmentation used to evaluate the GCC thickness: the inner and outer boundaries were set below the retinal nerve fiber layer and inner plexiform layer, respectively.

IS/OS reflectivity was associated with worse visual acuity in intermediate AMD eyes.¹³

Two of the challenges in using en face OCT to evaluate photoreceptor structure are the limited lateral resolution and the intrasubject factors that might influence the structure brightness and confound comparisons across a cohort. To solve the first problem, we tested the reflectivity in a circle region of interest centered on the fovea, excluding the scan edge. The second obstacle was overcome by “normalizing” the images—a technique we have successfully used in several prior reports.^{23–25} Our results showed no difference in the vitreous and RNFL reflectivity among groups, as well as a high-level intergrader reproducibility. Thus, our approach for generating a “normalized” reflectivity of the IS/OS slab would appear to be a reliable approach for assessing photoreceptor damage.

One previous study reported on the correlation between IS/OS band integrity and retinal sensitivity in AMD eyes. Landa and associates³⁶ enrolled 55 eyes of 43 consecutive patients with AMD, who underwent both SDOCT and microperimetry. The authors concluded that retinal

sensitivity consistently correlated with the status of the IS/OS junction in both early and late forms of AMD. Thus, the functional importance of the IS/OS or EZ in AMD eyes would appear to be well established.

We found that the IS/OS junction “normalized” reflectivity is significantly reduced in intermediate AMD eyes. We further divided our AMD cohort into 2 subgroups according to the GCC thickness. Interestingly, in this additional analysis, the reduction in IS/OS “normalized” reflectivity was still significant only in the abnormal GCC group. Importantly, the present study highlights the distinctive relationship between IS/OS “normalized” reflectivity and GCC thickness in intermediate AMD eyes: considering GCC thickness as dependent variable, we observed a direct relationship between these 2 variables, even after accounting for confounding factors, such as age and diabetes, which are known to modify GCC thickness.^{37,38} The absence of a relationship between GCC thickness and IS/OS “normalized” reflectivity in healthy subjects suggests the presence of a pathologic dysregulation in the AMD group. Assuming that GCC

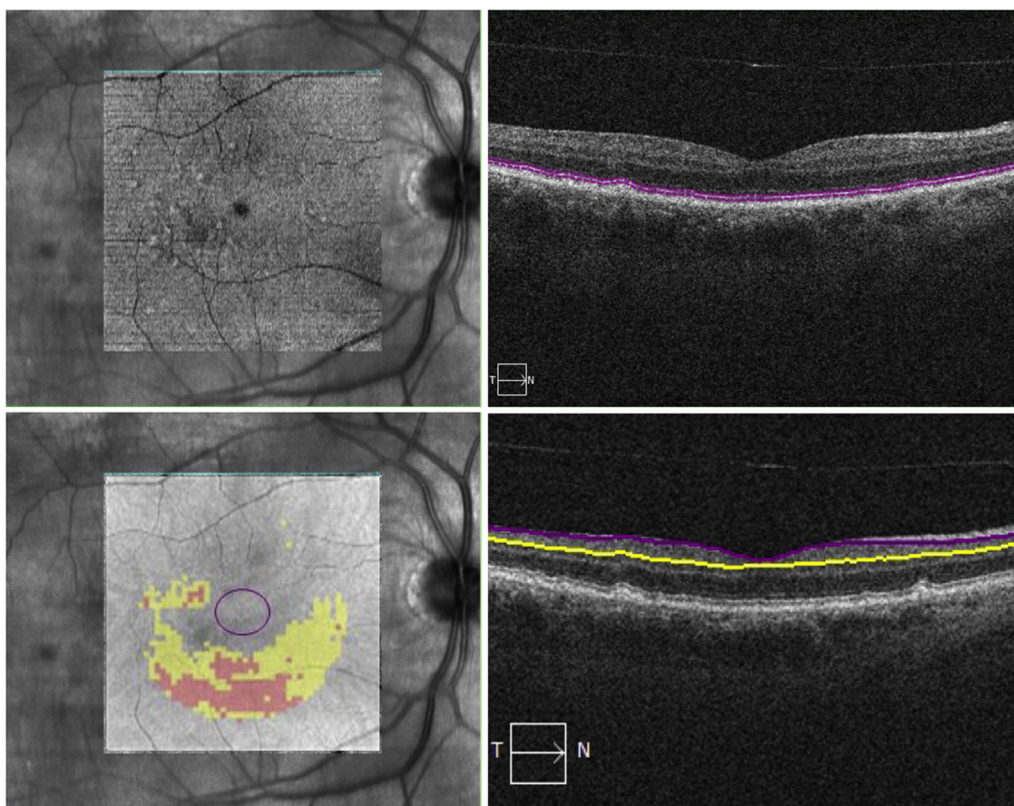


FIGURE 3. Representative optical coherence tomography (OCT) of a 71-year-old man from the abnormal ganglion cell complex (GCC) group. (Upper left) En face 6 × 6-mm inner segment/outer segment (IS/OS) junction OCT overlaid onto line-scan ophthalmoscope (LSO) fundus image. (Upper right) Corresponding OCT B-scan showing the slab set to visualize the IS/OS image: 21 μm thick with the inner boundary located 45 μm above the RPE reference. (Lower left) En face 6 × 6-mm structural OCT with GCC deviation map overlaid onto LSO fundus image. (Lower right) Corresponding OCT B-scan showing the segmentation used to evaluate the GCC thickness: the inner and outer boundaries were set below the retinal nerve fiber layer and inner plexiform layer, respectively.

thickness reduction is not the primary problem and cannot induce a secondary damage of the photoreceptors, and given that AMD is thought to be primarily an outer retina disease, we can speculate that our findings would appear to corroborate the postreceptor hypothesis as explanation for the observed inner retinal damage.

Another possible explanation for the reduced GCC thickness is mechanical tension to the inner retina caused by the elevation of the RPE and outer retina over drusen, leading to secondary retinal ganglion cell damage.⁸ Our results, however, would not seem to support this hypothesis, given that GCC thickness was not related to drusen area or volume.

The main limitation of our study is its retrospective and cross-sectional nature. A prospective longitudinal evaluation of the IS/OS reflectivity in intermediate AMD eyes should help shed further light on the role of the photoreceptor damage in the inner retinal layer thinning. Another limitation is that segmentation failure may occur when imaging eyes with AMD, resulting in erroneous measurements of the GCC thickness and segmentation of the IS/OS

slab.³⁹ We excluded such cases with artifacts from our analysis, but this may have given rise to a selection bias for our study. Another limitation of our study and approach is that thinning of the GCC may have itself resulted in altered reflectivity at the level of the IS/OS. We of course tried to account for differences in reflectivity of the RNFL itself (which turned out not to differ among the cohorts in this particular study) with our normalization approach, but this would not adjust for impact of thinner inner retina on the amount of signal transmitted to the deeper layers. One would expect, however, that with a thinner retina there would be an artifactually higher reflectivity of the deeper layers. In contrast, in our study we observed a reduced reflectivity at the level of IS/OS in AMD eyes with a thinner GCC. This reduction in reflectivity may have actually been an underestimate.

In conclusion, this study investigated the relationship between IS/OS “normalized” reflectivity and GCC thickness in eyes with intermediate AMD. We observed that eyes with intermediate AMD have GCC thinning, as well as reduced IS/OS “normalized” reflectivity, and these

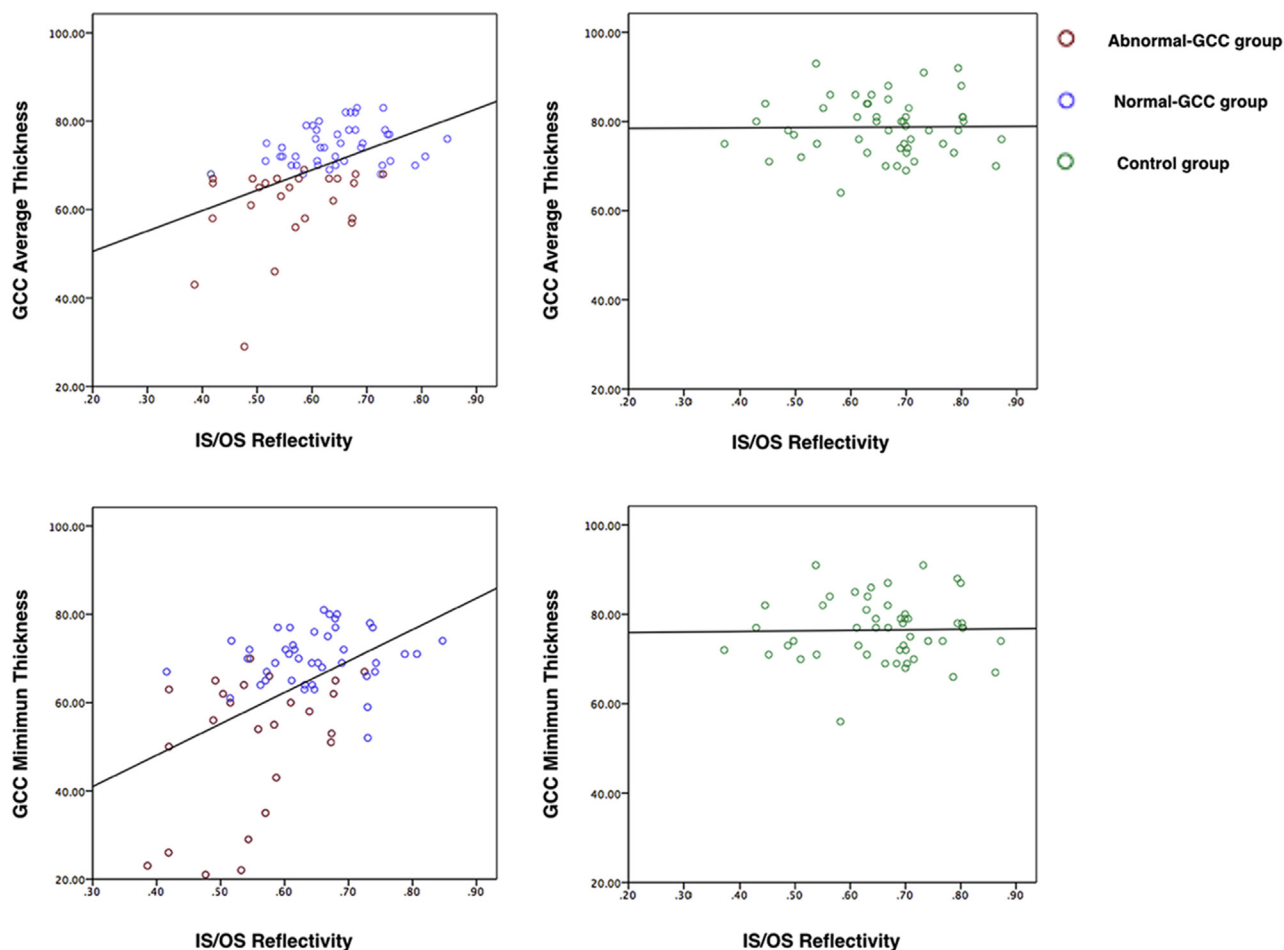


FIGURE 4. Scatterplots illustrating univariate regression analysis between the ganglion cell complex (GCC) thickness (set as dependent variable) and the inner segment/outer segment (IS/OS) “normalized” reflectivity. (Upper scatterplots) Relationship between average GCC thickness and IS/OS “normalized” reflectivity in age-related macular degeneration (AMD) patients ($P < .0001$) and controls ($P = .852$). (Lower scatterplots) Relationship between minimum GCC thickness and IS/OS “normalized” reflectivity in the AMD group ($P < .0001$) and in the control group ($P = .892$).

TABLE 4. Results of Multiple Regression Analysis of the Association Between Average Ganglion Cell Complex Thickness and Other Variables

	AMD		Control	
	Standardized β Coefficient (SE)	P Value	Standardized β Coefficient (SE)	P value
IS/OS “normalized” reflectivity	0.482 (10.526)	<.0001	-0.085 (8.764)	.594
Age	-0.222 (0.138)	.076	-0.240 (0.124)	.141
Sex	-0.013 (2.216)	.909	0.111 (1.847)	.448
Diabetes	-0.173 (0.256)	.109	-0.056 (0.377)	.625
Scan strength	-0.139 (0.841)	.239	-0.099 (0.748)	.528
Drusen area (mm ²)				
3-mm	-0.925 (11.188)	.212	-	-
5-mm	1.414 (10.600)	.110	-	-
Drusen volume (mm ³)				
3-mm	1.932 (276.551)	.079	-	-
5-mm	-2.280 (270.063)	.059	-	-

AMD = age-related macular degeneration; IS/OS = inner segment/outer segment junction; SE = standard error.

parameters appear to be related. These findings may help broaden our knowledge regarding the natural history of the disease and evolution of retinal neuronal loss. Lastly,

IS/OS junction “normalized” reflectivity, if replicated in future studies, may prove to be a useful biomarker for assessing the status of the retina in eyes with AMD.

FUNDING/SUPPORT: NO FUNDING OR GRANT SUPPORT. FINANCIAL DISCLOSURES: DAVID S. BOYER: AERPIO (CONSULTANT), Alcon (Consultant, Recipient), Allergan (Consultant, Recipient), Bayer (Consultant), Genentech (Consultant, Recipient), GS (Consultant), KalVista (Consultant), Neurotech (Consultant), Nicox (Consultant), Novartis (Consultant, Recipient), Ohr (Consultant), Santaris (Consultant), Santen (Consultant), ThromboGenics (Consultant), Regeneron Pharmaceuticals, Inc (Consultant, Recipient); SriniVas R. Sadda: Allergan (Consultant, Financial Support), Carl Zeiss Meditec (Financial Support), Genentech (Consultant, Financial Support), Iconic (Consultant), Novartis (Consultant), Optos (Consultant, Financial Support), Optovue (Consultant, Financial Support), Regeneron (Financial Support), Thrombogenics (Consultant). The following authors have no financial disclosures: Enrico Borrelli, Nizar Saleh Abdelfattah, Akihito Uji, and Muneeswar Gupta Nittala. All authors attest that they meet the current ICMJE criteria for authorship.

REFERENCES

1. Friedman DS, O'Colmain BJ, Muñoz B, et al. Prevalence of age-related macular degeneration in the United States. *Arch Ophthalmol* 2004;122(4):564–572.
2. Ferris FL, Wilkinson CP, Bird A, et al. Clinical classification of age-related macular degeneration. *Ophthalmology* 2013; 120(4):844–851.
3. Zarbin MA, Rosenfeld PJ. Pathway-based therapies for age-related macular degeneration: an integrated survey of emerging treatment alternatives. *Retina* 2010;30(9):1350–1367.
4. Querques G, Rosenfeld PJ, Cavallero E, et al. Treatment of dry age-related macular degeneration. *Ophthalmic Res* 2014; 52(3):107–115.
5. Curcio CA. Photoreceptor topography in ageing and age-related maculopathy. *Eye (Lond)* 2001;15(3):376–383.
6. Curcio CA, Messinger JD, Sloan KR, McGwin G, Medeiros NE, Spaide RF. Subretinal drusenoid deposits in non-neovascular age-related macular degeneration: morphology, prevalence, topography, and biogenesis model. *Retina* 2013;33(2):265–276.
7. Toto L, Borrelli E, Di Antonio L, Carpineto P, Mastropasqua R. Retinal vascular plexuses' changes in dry age-related macular degeneration, evaluated by means of optical coherence tomography angiography. *Retina* 2016;36(8): 1566–1572.
8. Lee EK, Yu HG. Ganglion cell–inner plexiform layer and peripapillary retinal nerve fiber layer thicknesses in age-related macular degeneration. *Invest Ophthalmol Vis Sci* 2015;56(6):3976–3983.
9. Hendrickson A, Warner CE, Possin D, Huang J, Kwan WC, Bourne JA. Retrograde transneuronal degeneration in the retina and lateral geniculate nucleus of the V1-lesioned marmoset monkey. *Brain Struct Funct* 2015;220(1):351–360.
10. Sullivan R, Penfold P, Pow DV. Neuronal migration and glial remodeling in degenerating retinas of aged rats and in nonneovascular AMD. *Invest Ophthalmol Vis Sci* 2003;44(2): 856–865.
11. Staurenghi G, Sadda S, Chakravarthy U, Spaide RF. International Nomenclature for Optical Coherence Tomography (IN·OCT) Panel. Proposed lexicon for anatomic landmarks in normal posterior segment spectral-domain optical coherence tomography: the IN·OCT consensus. *Ophthalmology* 2014;121(8):1572–1578.
12. Hood DC, Zhang X, Ramachandran R, et al. The inner segment/outer segment border seen on optical coherence tomography is less intense in patients with diminished cone function. *Invest Ophthalmol Vis Sci* 2011;52(13): 9703–9709.
13. Pappuru RR, Ouyang Y, Nittala MG, et al. Relationship between outer retinal thickness substructures and visual acuity in eyes with dry age-related macular degeneration. *Invest Ophthalmol Vis Sci* 2011;52(9):6743–6748.
14. Holladay JT. Proper method for calculating average visual acuity. *J Refract Surg* 1997;13(4):388–391.
15. Mwanza J-C, Oakley JD, Budenz DL, Chang RT, Knight OJ, Feuer WJ. Macular ganglion cell–inner plexiform layer: automated detection and thickness reproducibility with spectral domain–optical coherence tomography in glaucoma. *Invest Ophthalmol Vis Sci* 2011;52(11):8323–8329.
16. Kim KE, Jeoung JW, Park KH, Kim DM, Kim SH. Diagnostic classification of macular ganglion cell and retinal nerve fiber layer analysis. *Ophthalmology* 2015;122(3):502–510.
17. Nouri-Mahdavi K, Nowroozizadeh S, Nassiri N, et al. Macular ganglion cell/inner plexiform layer measurements by spectral domain optical coherence tomography for detection of early glaucoma and comparison to retinal nerve fiber layer measurements. *Am J Ophthalmol* 2013;156(6):1297–1307.e2.
18. Abdelfattah NS, Zhang H, Boyer DS, et al. Drusen volume as a predictor of disease progression in patients with late age-related macular degeneration in the fellow eye. *Invest Ophthalmol Vis Sci* 2016;57(4):1839–1846.
19. Yehoshua Z, Wang F, Rosenfeld PJ, Penha FM, Feuer WJ, Gregori G. Natural history of drusen morphology in age-related macular degeneration using spectral domain optical coherence tomography. *Ophthalmology* 2011;118(12): 2434–2441.
20. Hirasawa H, Araie M, Tomidokoro A, et al. Reproducibility of thickness measurements of macular inner retinal layers using SD-OCT with or without correction of ocular rotation. *Invest Ophthalmol Vis Sci* 2013;54(4):2562–2570.
21. Nittala MG, Ruiz-Garcia H, Sadda SR. Accuracy and reproducibility of automated drusen segmentation in eyes with non-neovascular age-related macular degeneration. *Invest Ophthalmol Vis Sci* 2012;53(13):8319–8324.
22. Carpineto P, Aharrh-Gnama A, Ciciarelli V, Mastropasqua A, Di Antonio L, Toto L. Reproducibility and repeatability of ganglion cell–inner plexiform layer thickness measurements in healthy subjects. *Ophthalmologica* 2014; 232(3):163–169.
23. Lee SY, Stetson PF, Ruiz-Garcia H, Heussen FM, Sadda SR. Automated characterization of pigment epithelial

- detachment by optical coherence tomography. *Invest Ophthalmol Vis Sci* 2012;53(1):164–170.
24. Charafeddin W, Nittala MG, Oregon A, Sadda SR. Relationship between subretinal hyperreflective material reflectivity and volume in patients with neovascular age-related macular degeneration following anti-vascular endothelial growth factor treatment. *Ophthalmic Surg Lasers Imaging Retina* 2015; 46(5):523–530.
 25. Hu Z, Nittala MG, Sadda SR. Comparison of retinal layer intensity profiles from different OCT devices. *Ophthalmic Surg Lasers Imaging Retina* 2013;44(6 Suppl):S5–S10.
 26. Kim SY, Sadda S, Pearlman J, et al. Morphometric analysis of the macula in eyes with disciform age-related macular degeneration. *Retina* 2002;22(4):471–477.
 27. Kim SY, Sadda S, Humayun MS, de Juan E, Melia BM, Green WR. Morphometric analysis of the macula in eyes with geographic atrophy due to age-related macular degeneration. *Retina* 2002;22(4):464–470.
 28. Savastano MC, Minnella AM, Tamburrino A, Giovinco G, Ventre S, Falsini B. Differential vulnerability of retinal layers to early age-related macular degeneration: evidence by SD-OCT segmentation analysis. *Invest Ophthalmol Vis Sci* 2014; 55(1):560–566.
 29. Zucchiatti I, Parodi MB, Pierro L, et al. Macular ganglion cell complex and retinal nerve fiber layer comparison in different stages of age-related macular degeneration. *Am J Ophthalmol* 2015;160(3):602–607.e1.
 30. Hwang YH. Patterns of macular ganglion cell abnormalities in various ocular conditions. *Invest Ophthalmol Vis Sci* 2014; 55(6):3995–4006.
 31. Toto L, Borrelli E, Mastropasqua R, et al. Association between outer retinal alterations and microvascular changes in intermediate stage age-related macular degeneration: an optical coherence tomography angiography study. *Br J Ophthalmol* 2017;101(6):774–779.
 32. Sallo FB, Peto T, Egan C, et al. “En face” OCT imaging of the IS/OS junction line in type 2 idiopathic macular telangiectasia. *Invest Ophthalmol Vis Sci* 2012;53(10):6145–6152.
 33. Oh J, Smiddy WE, Flynn HW, Gregori G, Lujan B. Photoreceptor inner/outer segment defect imaging by spectral domain OCT and visual prognosis after macular hole surgery. *Invest Ophthalmol Vis Sci* 2010;51(3):1651–1658.
 34. Villate N, Lee JE, Venkatraman A, Smiddy WE. Photoreceptor layer features in eyes with closed macular holes: optical coherence tomography findings and correlation with visual outcomes. *Am J Ophthalmol* 2005;139(2):280–289.
 35. Takahashi A, Ooto S, Yamashiro K, et al. Photoreceptor damage and reduction of retinal sensitivity surrounding geographic atrophy in age-related macular degeneration. *Am J Ophthalmol* 2016;168:260–268.
 36. Landa G, Su E, Garcia PMT, Seiple WH, Rosen RB. Inner segment-outer segment junctional layer integrity and corresponding retinal sensitivity in dry and wet forms of age-related macular degeneration. *Retina* 2011;31(2): 364–370.
 37. Bloch E, Yonova-Doing E, Jones-Odeh E, Williams KM, Kozareva D, Hammond CJ. Genetic and environmental factors associated with the ganglion cell complex in a healthy aging British cohort. *JAMA Ophthalmol* 2017;135(1): 31–38.
 38. Carpineto P, Toto L, Aloia R, et al. Neuroretinal alterations in the early stages of diabetic retinopathy in patients with type 2 diabetes mellitus. *Eye (Lond)* 2016;30(5):673–679.
 39. Hwang YH, Kim MK, Kim DW. Segmentation errors in macular ganglion cell analysis as determined by optical coherence tomography. *Ophthalmology* 2016;123(5):950–958.